Nanoscale

Accepted Manuscript

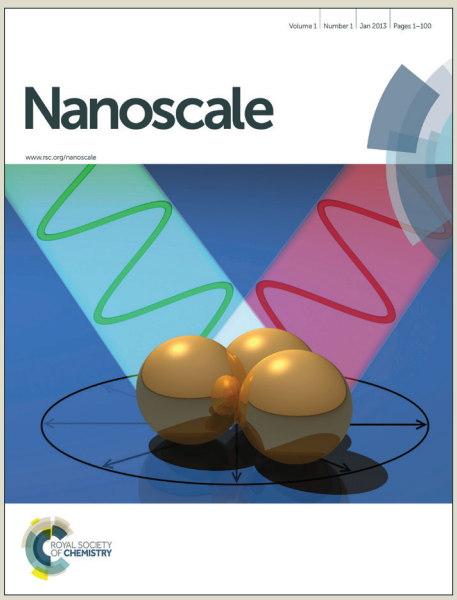

ROYAL SOCIETY OF CHEMISTRY

www.rsc.org/nanoscale

Comprehensive Interrogation of the Cellular Response to Fluorescent, Detonation and Functionalized Nanodiamonds

Laura Moore[1*], Valéria Grobárová[2*], Helen Shen[1], Han Bin Man[3], Júlia Míčová[4,5,$], Miroslav Ledvina[4,5], Jan Štursa[6], Milos Nesladek[5,7], Anna Fišerová[2,5**], Dean Ho[8,9**]

[1]Biomedical Engineering, Northwestern University, Evanston, Illinois, USA
[2]Institute of Microbiology, Czech Academy of Sciences, Prague, Czech Republic
[3]Mechanical Engineering, Northwestern University, Evanston, Illinois, USA
[4]Institute of Organic Chemistry and Biochemistry Academy of Sciences of the Czech Republic, v.v.i., Prague, Czech Republic
[5]The Faculty of Biomedical Engineering, Czech Technical University in Prague, Kladno, Czech Republic
[6]Nuclear Physics Institute, Academy of Sciences of the Czech Republic, v.v.i., 250 68, Rez near Prague, Czech Republic
[7]Institute for Materials Research (IMO), Hasselt University, Hasselt, Belgium
[8]Division of Oral Biology and Medicine, Division of Advanced Prosthodontics, The Jane and Jerry Weintraub Center for Reconstructive Biotechnology, UCLA School of Dentistry, Los Angeles, California, USA
[9]Department of Bioengineering, Jonsson Comprehensive Cancer Center, California NanoSystems Institute, UCLA, Los Angeles, California, USA

*these authors contributed equally to this work.
**co-corresponding authors

Table of Contents:

Nanodiamonds are versatile nanoparticles that are currently being investigated in a multitude of different formulations. These studies evaluate the cellular response to four of the most promising subtypes: fluorescent, detonation, functionalized and drug loaded nanodiamonds.

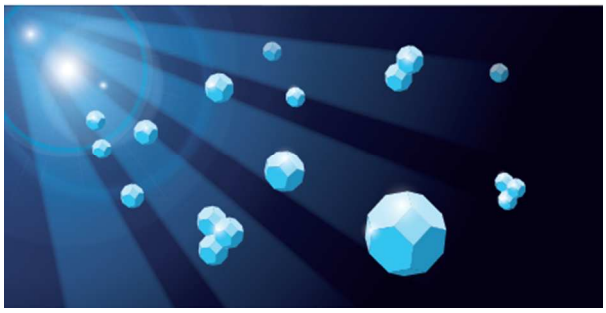

[$]Permanent address: Institute of Chemistry, Slovak Academy of Science, 845 38 Bratislava, Slovak Republic

Abstract:

Nanodiamonds (NDs) are versatile nanoparticles that are currently being investigated for a variety of applications in drug delivery, biomedical imaging and nanoscale sensing. Although initial studies indicate that these small gems are biocompatible, there is a great deal of variability in synthesis methods and surface functionalization that has yet to be evaluated. Here we present a comprehensive analysis of the cellular compatibility of an array of nanodiamond subtypes and surface functionalization strategies. These results demonstrate that NDs are well tolerated by multiple cell types at both functional and gene expression levels. In addition, ND-mediated delivery of daunorubicin is less toxic to multiple cell types than treatment with daunorubicin alone, demonstrating the ability of the ND agent to improve drug tolerance and decrease therapeutic toxicity. Overall, the results here indicate that ND biocompatibility serves as a promising foundation for continued preclinical investigation.

1. Introduction:

In recent years nanomaterials have been gaining popularity in biomedical applications, particularly in the drug delivery and biomedical imaging arenas. This boom is at least in part due to their ability to improve both physical properties and biological activity or imaging contrast. One particularly promising nanomaterial is the nanodiamond (ND).[1, 2] NDs are faceted carbon nanoparticles that contain a diamond crystal structure. To date NDs have been used to deliver a wide variety of bioactive molecules including polymers,[3, 4] proteins,[5-7] nucleic acids,[8-10] vitamins,[11] small-molecule therapeutics[12-15] and contrast agents.[16, 17] NDs can additionally be used as fluorescent labels [18-21] and nanoscale magnetic field sensors.[22]

Thus far the results from preclinical efficacy studies of NDs have been extremely promising.[23] The next step towards clinical translation of NDs is the assessment of their biocompatibility. Preliminary studies of NDs indicate that they are extremely well tolerated.[3, 12, 20, 24-28] However, there are a few studies that indicate that NDs may have a negative impact on certain cell types.[29, 30] Additionally, within the category of NDs there is a great deal of variability in synthesis method, size and surface functionalization.[1, 31] Depending on the synthesis method size alone can vary from 3nm up to nearly a micron, which can have a large impact on particle properties.[32] We also see variation in surface functional groups, shape and ζ-potential depending on the synthesis method (Table 1). With the wide range of particles that can claim the title “ND” there a need to better understand of the impact of the differing particle subtypes and surface modifications.

To the best of our knowledge, this is the first study to examine the cellular impact of the differing subtypes of NDs. Here we have chosen to evaluate the cellular response to 4 common types of ND: unmodified detonation NDs (dNDs), amine-functionalized dNDs (aNDs), daunorubicin functionalized dNDs (ND-DNR) and fluorescent NDs (fNDs) (Table 1, Figure 1). dNDs are 4-5nm particles that form a stable colloidal solution with cluster sizes averaging 35-50nm. Among other therapeutic and biomedical imaging agents, dNDs serve as the foundation for the ND-doxorubicin,[12, 15, 25, 33] ND-lipid hybrid particles[13] and ND-based MRI contrast agents.[16] The synthesis of dNDs leaves them with a variety of oxygen-containing, surface functional groups (Figure 1A, dNDs) that can be modified for covalent functionalization. dNDs are also commonly modified, through reduction and coupling to (3-aminopropyl)triethoxysilane,[34] to generate similarly sized NDs with primary amines on the surface (Figure 1, aNDs). aNDs serve as the reactive foundation for a variety of modified NDs, including fluorophore conjugated NDs[12, 13] and multimodal NDs.[9]

Alternatively, dNDs can be non-covalently functionalized with a variety of therapeutic molecules,[35] including anthracycline chemotherapeutics.[12] Similar to doxorubicin loaded NDs, ND-DNR is generated by adsorption of daunorubicin into dND clusters (Figure 1, ND-DNR).[36] One of the major advantages of ND-mediated delivery of anthracycline chemotherapeutics is that they overcome cellular resistance mechanisms.[12, 36] Additionally, ND-doxorubicin reduces the side effects of doxorubicin, thereby improving overall drug safety. Here we have chosen to study ND-daunorubicin, which has been shown to overcome cellular resistance mechanisms in leukemia cells.[36]

Finally, we also chose to compare to innately fluorescent NDs, which are not synthesized from dNDs. The fNDs studied here are approximately 45nm particles (Figure 1, fNDs) that that are innately fluorescent due to nitrogen vacancies (NV) in the diamond crystal structure.[37] These can be synthesized in a variety of fashions, but are generally larger than dNDs due to the need for additional NV centers to generate brighter fluorescence.[38-41] Previous reports have assessed

the biocompatibility of fluorescent nanodiamonds alone,[42, 43] and have found that they do not alter cell viability. However, the particles previously studied represent a separate subset of even larger fNDs (145nm) and have not been comprehensively analyzed or directly compared to other NDs.

Here we present the most comprehensive analysis of cellular compatibility of NDs to date and the first to compare multiple ND subtypes. These results demonstrate that even all ND subtypes are well tolerated by multiple cell types and have minimal impact on cellular metabolism, cell death, apoptosis induction and gene expression, even at supra-therapeutic levels. These results confirm that at a fundamental level diamond nanoparticles are extremely biocompatible and serves as the foundation for future preclinical studies.

2. Materials and Methods:

2.1. Materials

All materials were acquired from Life Technologies (Carlsbad, CA, USA) unless otherwise specified. Detonation nanodiamonds were purchased from the Nanocarbon Research Institute (Nagano, Japan). High pressure high temperature (HPHT) nanodiamonds average size 45 nm contained about 100-120 ppm nitrogen, i.e., starting material for preparation of fluorescent nanodiamond, were sourced from Microdiamant AG, Switzerland. HepG2 and HeLa cells were acquired from ATCC (Manassas, VA, USA). Cell culture media and supplements were acquired from VWR (Radnor, PA, USA). Caspase Glo-3/7 and Cytotox 96 were acquired from Promega Corporation (Madison, WI, USA). Daunorubicin was acquired from Sigma-Aldrich (St. Louis, MO, USA).

2.2. ND-Synthesis

Amine modified NDs (aND) were synthesized according to the protocol originally described by Kruger, et al.[44] Briefly, lyophilized NDs (2.5g) were reduced with BH3•THF (25mL, 1M) for 3 days followed by functionalization (1g) with (3-aminopropyl) trimethoxysilane (100mL, 5%). After washing and lyophilization aNDs were suspended in 0.2% acetic acid using probe sonication. ND-daunorubicin was synthesized using the protocol described by Man *et al*.[36] Briefly, dNDs (1mg/mL) are combined with daunorubicin (0.2mg/mL) in the presence of sodium hydroxide (2.5mM) and allowed to precipitate overnight. ND-DNR clusters are then collected by centrifugation and resuspended in water using probe sonication, forming a stable colloidal solution.

2.3. fND-Preparation

A surface graphite contamination of commercial HPHT NDs was removed by two step oxidation, i.e., by heating in air atmosphere at 450 °C for 6 h and subsequent heating in a mixture of concentrated H_2SO_4-HNO_3 (9:1, v/v) at 90 °C for 3 days. The reaction mixture was diluted with deionized water and the NDs were separated by centrifugation and washed subsequently with 0.1 M NaOH, 0.1 M HCl, and finally three times with MilliQ water than lyophilized from MilliQ water. The obtained NDs were dispersed in water and deposited in the form of a thin film on a target backing (10 mg cm−2) for proton implantation. The ND film was then irradiated using an external proton beam of the isochronous cyclotron U-120M. The angle of the target backing with respect to the beam direction was 10°. The fluence of the delivered beam was 9.2 × 1015 cm−2, the beam energy was 5.4 MeV, and the beam current was 0.6 μA. The irradiated NDs were thermally annealed in inert atmosphere at 900°C for 1 hour to form either neutral (NV^0) and negatively charged (NV^-) centers.[41] The graphene-like impurities resulting from irradiation and annealing were finally removed by oxidation with air at 450 °C for 6 h. Dominant chemical functions presented on the surface such prepared fNDs are carboxyl and primary hydroxyl groups and ketones (Figure 1, fNDs).

2.4. Cell culture

Cells were cultured in DMEM supplemented with 10% fetal bovine serum (FBS) and 1% penicillin-streptomycin in a humidified atmosphere at 37°C with 5% CO_2. Cells were seeded in flat-bottom 96-well plates at $2.5x10^4$ cells per well and cultured in a final volume of 200µl DMEM supplemented with 10% FBS and 1% penicillin-streptomycin. Cells were incubated with varying concentrations (1µg/mL-1mg/ml) of plain NDs, amine-modified NDs, fluorescent NDs or daunorubicin-loaded NDs for either 4 (ND-Daunorubicin) or 24 hours (all others). As amine modified NDs were suspended in 0.2% acetic acid, an equivalent volume of 0.2% acetic acid was added to negative controls. After the incubation period 100µl of media was removed from each well and transferred to a new plate for the LDH release assay.

2.5. XTT Assay

For the XTT assay untreated cells were used as a negative control and 1% SDS as a positive control. 50µl of XTT reaction mixture (100µg/mL XTT reagent, 25µM menadione in phosphate buffered saline) was added to each well. After 2 hours incubation at 37°C absorbance was measured at 475nm using a Biotek Synergy 4 or SpectraMax M5 plate reader. Absorbance was normalized to a reference wavelength (600nm) and background subtracted using wells with test material but no cells.

2.6. Caspase 3/7 Activation Assay

For the caspase activation assay 1-4µM staurosporine, incubated for 4 hours, was used as a positive control and untreated cells the negative control. 50µl of substrate mix (Promega CaspaseGlo 3/7 Assay) was added to each well and incubated for 30 minutes at 37°C. Luminescence was measured using a Biotek Synergy 4 or SpectraMax M5 plate reader.

2.7. LDH Release Assay

Lactate dehydrogenase (LDH) release from cells was measured in culture supernantants from either the XTT or caspase activation assays. Cells were incubated with the cell lysis solution (Promega Cytotox 96 kit) for 45 minutes to obtain a positive control while untreated cells were used as a negative control. 50µl of supernatant from each well was transferred to a fresh 96-well plate and combined with 50µl of reconstituted Substrate Mix (kit). Plates were incubated for 30 minutes at room temperature for 30 minutes prior to adding 50µl of stop solution (kit). Absorbance was read at 490nm on a Biotek Synergy 4 or SpectraMax M5 plate reader. Absorbance was compared to a reference wavelength (690nm) and background subtracted using wells with test material but no cells.

2.8. Reverse transcription quantitative real-time PCR (RT-qPCR)

HepG2 and HeLa cell lines (400,000/well) were treated with 25 µg/ml of dNDs, aND or fNDs for 24 hours. As a positive control campthotecin with concentration 1mM or 5 mg/mL was used. Total RNA from cells was extracted using the Trizol (Life Technologies), following manufactures protocol. 100 ng of RNA were transcribed into cDNA using the cDNA Archive Kit (Applied Biosystem, Foster City, CA, USA). RT-qPCR analysis for *Bax, COX-2, c-Myc*, and *Ki-67* genes was carried out with a TaqMan probes and TaqMan Gene Expression Master Mix (Applied Biosystem) using an iCycler5 (Bio-Rad, Hercules, CA, USA). The genes were normalized to the reference gene (*GAPDH*). Differences in gene expression were evaluated by the ΔΔCt method with GenEx Pro software version.

2.9. Statistical Analysis

All experiments were conducted with a minimum 3 replicates. Statistics for XTT, LDH release and caspase 3/7 activation assays were performed in GraphPad Prism a two-way ANOVA and

the Bonferroni correction for multiple comparisons. Statistics for PCR analysis was completed using GenEx software and a paired t-test (two-tailed).

3. Results

3.1. Cellular impact of modified and unmodified detonation nanodiamonds

The impact of dNDs and aNDs was first assessed on two cancer cell lines: HepG2 (hepatocellular carcinoma) and HeLa (cervical adenocarcinoma). The two cell lines were selected because they are broadly used and representative of different germ layers: endoderm and ectoderm. Varying concentrations of dNDs or aNDs were incubated with both cell lines for 24 hours prior to assaying for metabolic activity (XTT assay), cell death (lactate dehydrogenase release) or apoptosis (caspase 3/7 activation) (Figure 2). These results demonstrate that neither dNDs nor aNDs diminish cell metabolic activity in the HepG2s (Figure 2A). At the very highest concentrations (1mg/ml) both dNDs and aNDs induce a modest increase in cell death (Figure 2C) and apoptosis (Figure 2E). However, the lack of impact on metabolic activity indicates that overall the overall impact on the culture is minimal.

In contrast to the HepG2s, at the highest concentrations (1mg/ml) the dNDs and aNDs induce a modest reduction in cell metabolic activity in the HeLa cells (Figure 2B). However, this effect was not accompanied by an increase in cell death (Figure 2D) or apoptosis (Figure 2F). Taken together these results indicate that at extreme concentrations dNDs and aNDs may inhibit proliferation in the HeLa cells. However, at more reasonable concentrations (<500μg/ml) neither the dNDs nor the aNDs had any effect on cellular metabolism, cell death or caspase activation in either cell line.

3.2. Cellular impact of fluorescent nanodiamonds

fNDs were synthesized by proton beam irradiation of high temperature, high pressure (HPHT) diamond nanocrystals followed by annealing at 900°C for 1 hour. The resulting fNDs were assessed in a similar fashion to the dNDs and aNDs. Varying concentrations of fNDs were incubated with HeLa or HepG2 cells for 24 hours prior to assaying for cellular metabolic activity (XTT) and overall cell death (LDH release). Due to a limited supply of fNDs we were unable to complete additional assays or test extreme concentrations. However, this assessment indicates that fNDs are extremely well tolerated by both cell lines (Figure 3). HepG2 cells treated with fNDs do not show any alterations in cell metabolic activity (Figure 3A) or cell death (Figure 3C). The same was observed with the HeLa cells (Figures 3B, D respectively). These results indicate that in spite of the larger size and differing synthesis method the fNDs are still extremely well tolerated.

3.3. Transcriptional response to ND-treatment

In order to more precisely assess the impact that the dNDs, aNDs and fNDs had on cells their transcriptional response to the NDs was probed using RT-qPCR. In the HepG2 cells 3 different transcripts as indicators of cell health were assessed: *Bax* (pro-apoptosis), *c-Myc* (anti-apoptosis, pro-proliferation) and *Ki-67* (pro-proliferation). HepG2 cells were incubated with 25μg/ml of dNDs, aNDs or fNDs for 24 hours prior to recovery of genetic material. We observe that none of the ND-subtypes induce increases in *Bax* expression in the HepG2 cells (Figure 4A), which is indicative of a lack of apoptosis response. In addition, we find that ND treatment does not down-regulate *c-Myc* (Figure 4B), which suggests the NDs do not inhibit cellular proliferation or induce apoptosis. Furthermore, probing *Ki-67* confirms that the NDs do not induce an anti-proliferative response in the HepG2 cells (Figure 4C). When combined with the results in Figures 2 and 3, these results indicate that none of the 3 ND-subtypes tested induces a toxic response in the HepG2 cells.

Similar to the HepG2s, HeLa cells were incubated with 25µg/mL of dNDs, aNDs and fNDs and probed for alterations in gene expression. ND treatment did not induce alterations in the expression of *Bax*, (Figure 5A), *c-Myc* (Figure 5B) or *Ki-67* (Figure 5C) in the HeLa cells, which is consistent with Figures 2 and 3. However, in addition to *Bax*, *c-Myc* and *Ki-67*, *COX-2* was probed in the HeLa cells to assess the inflammatory response to the differing ND-subtypes. Because *COX-2* is frequently overexpressed in hepatocellular carcinoma we elected not to probe its expression in the HepG2 cells. Treatment of HeLa cells with each of the 3 ND-subtypes failed to up-regulate *COX-2* expression (Figure 5D), indicating a lack inflammatory response. This work demonstrates that at 25µg/ml dNDs, aNDs and fNDs do not promote apoptosis, induce an inflammatory response or inhibit proliferation in the HeLa cells.

3.4. Cellular treatment with ND-Daunorubicin

One of the major advantages of dNDs as a drug delivery vehicle is their ability to deliver anthracycline chemotherapeutics in a controlled manner. Previous work on nanodiamond doxorubicin demonstrates that nanodiamond-mediated delivery of doxorubicin increases drug circulation time, promotes tumor localization, overcomes chemoresistance and virtually eliminates drug toxicities.[12] Here we evaluate the cellular response to ND delivery of daunorubicin, an anthracycline chemotherapeutic closely related to doxorubicin. Early studies of ND-daunorubicin have demonstrated that it can overcome resistance mechanisms in leukemia cells.[36] ND-DNR was synthesized in the same manner as ND-doxorubicin[12] and ND-epirubicin.[13] Release of daunorubicin from ND-clusters is pH dependent and takes place over the first 6-12 hours. For this reason,[36] HepG2 and HeLa cells were treated with 10-100µg/ml of DNR as ND-DNR or free daunorubicin for 4 hours prior to assaying for cellular metabolic activity, cell death and initiation of apoptosis (Figure 6). HepG2 cells show increased metabolic activity with ND-DNR (Figure 6A, ANOVA $p=0.0004$), reduced cell death (Figure 6C, ANOVA $p<0.0001$) and less apoptosis (Figure 6E, ANOVA $p<0.0001$). The HeLa cells responded similarly, with ND-DNR treatment showing improved cell metabolic activity compared to free daunorubicin (Figure 6B, ANOVA $p=0.012$), diminished cell death (Figure 6D, ANOVA $p<0.0001$), and reduced apoptosis (Figure 6F, ANOVA $p=0.0014$). Because neither cell line is resistant to daunorubicin these results are extremely promising. Overall this work shows that ND-DNR is less toxic than the equivalent dose free daunorubicin to both epithelial and liver cells, which are two of the cell types hardest hit by conventional chemotherapeutics.

4. Discussion:

One of the biggest challenges with developing new nanomaterials for biomedical applications is that in order to be clinically useful the material must be biocompatible and well tolerated. Although many nanoparticles may be well tolerated by cells and animals when pristine, there are limited studies assessing their biological impact when modified. This is particularly true for NDs, which can be synthesized and modified using a variety of methods to produce vast array of subtypes and surface chemistries. Here have strived to complete a comprehensive analysis of the cellular response to different types and modifications of NDs.

Previous work on ND biocompatibility has primarily focused on cell viability after dND treatment in comparison to other nanoparticles.[24] Although there are more detailed studies of the cellular response to dNDs alone,[25] there is little information available comparing dNDs to other ND subtypes. Additionally, some of the results in the literature present conflicting information on dND genotoxicity.[28, 29] Because NDs are finding increasing usage in both modified and unmodified forms, an in depth understanding of their impact on cells is necessarily for their clinical and commercial translation. Of the ND subtypes, aNDs and fNDs are some of the most commonly utilized. aNDs are a especially important subtype to study due to the frequency of

their use as a foundation for other functionalized NDs. The studies of aNDs are crucial because of the high toxicity of other materials presenting excess primary amines, such as poly-lysine. Furthermore, because nanoparticle size has a strong impact on their interaction with cells,[45] the studies comparing the larger fNDs to the smaller dNDs are particularly informative.

Overall these studies have found that non-therapeutic NDs are extremely well tolerated by liver and epithelial cell lines even at supra-therapeutic doses (Figures 2 and 3). For comparison, mice treated with an aggressive dose of doxorubicin (100μg) would experience a maximum concentration of 250μg/ml NDs in circulation immediately after injection, which would rapidly diminish as the NDs distribute. At 250μg/ml all the non-therapeutic ND types are exceptionally well tolerated by both cell types, suggesting that they should also be well tolerated *in vivo.*

For the gene expression studies NDs were tested at a lower concentration, 25μg/mL, to more closely mimic the concentration organs might see after ND distribution from the blood stream. These studies demonstrate that treatment with dNDs, aNDs or fNDS does not induce changes in the expression of genes involved in apoptosis, cellular proliferation or inflammation (Figures 4 and 5). These findings are important because it is possible for cells to be functionally normal while still exhibiting changes in gene expression. However, this work shows that treatment with NDs of any subtype did not induce significant changes in cell metabolism, proliferation or apoptosis at either the functional or gene expression level.

In addition to being non-toxic to the two cell types tested, NDs are capable of reducing the toxicity of the anthracycline chemotherapeutic daunorubicin. When daunorubicin is delivered by NDs to either HepG2 or HeLa cells it is less toxic than when delivered as a free acid. This effect is expected and beneficial as neither the HepG2 nor HeLa cells are resistant to daunorubicin. Liver and epithelial cells, like HepG2 and HeLas, are two of the cell types most negatively affected by chemotherapy. Because ND-DNR is less toxic to these two cell types than free daunorubicin, this work suggests ND-mediated delivery of daunorubicin may improve the side effect profile of daunorubicin if used *in vivo*.

5. Conclusions

In conclusion, the comprehensive assessment of cellular compatibility presented in this work shows that NDs synthesized in different manners and carrying differing surface functionalizations are well tolerated by multiple cell types. Additionally, these results demonstrate that daunorubicin is less toxic to multiple cell types when delivered by ND. Combined these results demonstrate that NDs are extremely promising vehicles for drug delivery and merit further pre-clinical evaluation.

6. Acknowledgements:

The authors gratefully acknowledge support from European Commission funding program FP7-KBBE-2009-3,Grant No. 245122. In addition, D.H. gratefully acknowledges support from the National Science Foundation CAREER Award (CMMI-1350197), Center for Scalable and Integrated NanoManufacturing (DMI-0327077), CMMI-0856492, DMR-1343991, V Foundation for Cancer Research Scholars Award, Wallace H. Coulter Foundation Translational Research Award, Society for Laboratory Automation and Screening Endowed Fellowship, and Beckman Coulter. D.H. and L.M. gratefully acknowledge support from National Cancer Institute grant U54CA151880 (The content is solely the responsibility of the authors and does not necessarily represent the official views of the National Cancer Institute or the National Institutes of Health). L.M. gratefully acknowledges support from the National Cancer Institute Grant 1F30CA174156 and the Northwestern University Malkin Scholarship. Additionally, this work was facilitated by core facilities provided by the Northwestern University Institute for Bionanotechnology and

Medicine and the Northwestern University Atomic and Nanoscale Expermental Center. V.G. and A.F. gratefully acknowledge the support of Institutional Research Concept (RVO 61388971). M.L. appreciate the support Institutional Research Concept (RVO 61388963). J.S. acknowledges the support Institutional Research Concept (RVO 61389005) and the CANAM infrastructure of the NPI ASCR Rez supported through MEYS, project No. LM2011019.

References

1. V. N. Mochalin, O. Shenderova, D. Ho and Y. Gogotsi, *Nat. Nano.*, 2012, **7**, 11-23.
2. E. Perevedentseva, Y. C. Lin, M. Jani and C. L. Cheng, *Nanomedicine (Lond)*, 2013, **8**, 2041-2060.
3. Z. Xing, T. O. Pedersen, X. Wu, Y. Xue, Y. Sun, A. Finne-Wistrand, F. R. Kloss, T. Waag, A. Krueger, D. Steinmuller-Nethl and K. Mustafa, *Tissue Eng. Part A*, 2013, **19**, 1783-1791.
4. I. Rehor, J. Slegerova, J. Kucka, V. Proks, V. Petrakova, M.-P. Adam, F. Treussart, S. Turner, S. Bals, P. Sacha, M. Ledvina, A. M. Wen, N. F. Steinmetz and P. Cigler, *Small*, 2014, n/a-n/a.
5. A. H. Smith, E. M. Robinson, X. Q. Zhang, E. K. Chow, Y. Lin, E. Osawa, J. Xi and D. Ho, *Nanoscale*, 2011, **3**, 2844-2848.
6. R. A. Shimkunas, E. Robinson, R. Lam, S. Lu, X. Xu, X.-Q. Zhang, H. Huang, E. Osawa and D. Ho, *Biomaterials*, 2009, **30**, 5720-5728.
7. C. M. F. Liu K K, Chen P Y, Lee T J F, Cheng C L, Chang C C, Ho Y P and C. J. I, *Nanotechnology*, 2008, **19**, 205102.
8. M. Chen, X.-Q. Zhang, H. B. Man, R. Lam, E. K. Chow and D. Ho, *J. Phys. Chem. Lett.*, 2010, **1**, 3167-3171.
9. X.-Q. Zhang, R. Lam, X. Xu, E. K. Chow, H.-J. Kim and D. Ho, *Adv. Mater.*, 2011, 4770–4775.
10. X. Q. Zhang, M. Chen, R. Lam, X. Xu, E. Osawa and D. Ho, *ACS Nano*, 2009, **3**, 2609-2616.
11. A. Krueger, J. Stegk, Y. Liang, L. Lu and G. Jarre, *Langmuir*, 2008, **24**, 4200.
12. E. K. Chow, X.-Q. Zhang, M. Chen, R. Lam, E. Robinson, H. Huang, D. Schaffer, E. Osawa, A. Goga and D. Ho, *Sci. Trans. Med.*, 2011, **3**, 73ra21.
13. L. Moore, E. K. Chow, E. Osawa, J. M. Bishop and D. Ho, *Adv. Mater.*, 2013.
14. H.-J. Kim, K. Zhang, L. Moore and D. Ho, *ACS Nano*, 2014.
15. J. Xiao, X. Duan, Q. Yin, Z. Zhang, H. Yu and Y. Li, *Biomaterials*, 2013, **34**, 9648-9656.
16. L. M. Manus, D. J. Mastarone, E. A. Waters, X. Q. Zhang, E. A. Schultz-Sikma, K. W. Macrenaris, D. Ho and T. J. Meade, *Nano Lett.*, 2010, **10**, 484-489.
17. H. A. Girard, A. El-Kharbachi, S. Garcia-Argote, T. Petit, P. Bergonzo, B. Rousseau and J.-C. Arnault, *Chem. Commun.*, 2014, **50**, 2916-2918.
18. V. N. Mochalin and Y. Gogotsi, *J. Am. Chem. Soc.*, 2009, **131**, 4594-4595.
19. Q. Zhang, V. N. Mochalin, I. Neitzel, I. Y. Knoke, J. Han, C. A. Klug, J. G. Zhou, P. I. Lelkes and Y. Gogotsi, *Biomaterials*, 2011, **32**, 87-94.
20. N. Mohan, C.-S. Chen, H.-H. Hsieh, Y.-C. Wu and H.-C. Chang, *Nano Lett.*, 2010, **10**, 3692-3699.
21. V. Petráková, A. Taylor, I. Kratochvílová, F. Fendrych, J. Vacík, J. Kučka, J. Štursa, P. Cígler, M. Ledvina, A. Fišerová, P. Kneppo and M. Nesládek, *Adv. Funct. Mater.*, 2012, **22**, 812-819.
22. G. Balasubramanian, I. Y. Chan, R. Kolesov, M. Al-Hmoud, J. Tisler, C. Shin, C. Kim, A. Wojcik, P. R. Hemmer, A. Krueger, T. Hanke, A. Leitenstorfer, R. Bratschitsch, F. Jelezko and J. Wrachtrup, *Nature*, 2008, **455**, 648-651.

23. E. K.-H. Chow and D. Ho, *Sci. Trans. Med.*, 2013, **5**, 216rv214.
24. X. Zhang, W. Hu, J. Li, L. Tao and Y. Wei, *Toxicol. Res.*, 2012, **1**, 62-68.
25. H. Huang, E. Pierstorff, E. Osawa and D. Ho, *Nano Lett.*, 2007, **7**, 3305.
26. S. J. Yu, M. W. Kang, H. C. Chang, K. M. Chen and Y. C. Yu, *J. Am. Chem. Soc.*, 2005, **127**, 17604.
27. Y. Yuan, X. Wang, G. Jia, J.-H. Liu, T. Wang, Y. Gu, S.-T. Yang, S. Zhen, H. Wang and Y. Liu, *Diamond Relat. Mater.*, 2010, **19**, 291-299.
28. V. Paget, J. A. Sergent, R. Grall, S. Altmeyer-Morel, H. A. Girard, T. Petit, C. Gesset, M. Mermoux, P. Bergonzo, J. C. Arnault and S. Chevillard, *Nanotoxicology*, 2013.
29. Y. Xing, W. Xiong, L. Zhu, E. Osawa, S. Hussin and L. Dai, *ACS Nano*, 2011, **5**, 2376-2384.
30. L. Marcon, F. Riquet, D. Vicogne, S. Szunerits, J.-F. Bodart and R. Boukherroub, *J. Mater. Chem.*, 2010, **20**, 8064-8069.
31. L. Zhao, T. Takimoto, M. Ito, N. Kitagawa, T. Kimura and N. Komatsu, *Angew. Chem. Int. Ed. Engl.*, 2011, **50**, 1388-1392.
32. A. S. Barnard and E. Osawa, *Nanoscale*, 2014, **6**, 1188-1194.
33. G. Xi, E. Robinson, B. Mania-Farnell, E. F. Vanin, K. W. Shim, T. Takao, E. V. Allender, C. S. Mayanil, M. B. Soares, D. Ho and T. Tomita, *Nanomedicine*, 2014, **10**, 381-391.
34. A. Kruger, Y. J. Liang, G. Jarre and J. Stegk, *J. Mater. Chem.*, 2006, **16**, 2322.
35. M. Chen, E. D. Pierstorff, R. Lam, S.-Y. Li, H. Huang, E. Osawa and D. Ho, *ACS Nano*, 2009, **3**, 2016-2022.
36. H. B. Man, H. Kim, H. J. Kim, E. Robinson, W. K. Liu, E. K. Chow and D. Ho, *Nanomedicine*, 2013.
37. J.-P. Boudou, P. A. Curmi, F. Jelezko, J. Wrachtrup, P. Aubert, M. Sennour, G. Balasubramanian, R. Reuter, A. Thorel and E. Gaffet, *Nanotechnology*, 2009, **20**, 235602.
38. J. R. Rabeau, A. Stacey, A. Rabeau, S. Prawer, F. Jelezko, I. Mirza and J. Wrachtrup, *Nano Lett.*, 2007, **7**, 3433-3437.
39. J. Tisler, G. Balasubramanian, B. Naydenov, R. Kolesov, B. Grotz, R. Reuter, J.-P. Boudou, P. A. Curmi, M. Sennour, A. Thorel, M. Börsch, K. Aulenbacher, R. Erdmann, P. R. Hemmer, F. Jelezko and J. r. Wrachtrup, *ACS Nano*, 2009, **3**, 1959-1965.
40. C. Bradac, T. Gaebel, N. Naidoo, J. R. Rabeau and A. S. Barnard, *Nano Lett.*, 2009, **9**, 3555-3564.
41. J. Havlik, V. Petrakova, I. Rehor, V. Petrak, M. Gulka, J. Stursa, J. Kucka, J. Ralis, T. Rendler, S. Y. Lee, R. Reuter, J. Wrachtrup, M. Ledvina, M. Nesladek and P. Cigler, *Nanoscale*, 2013, **5**, 3208-3211.
42. V. Vaijayanthimala and H. C. Chang, *Nanomedicine (Lond)*, 2009, **4**, 47-55.
43. V. Vaijayanthimala, P. Y. Cheng, S. H. Yeh, K. K. Liu, C. H. Hsiao, J. I. Chao and H. C. Chang, *Biomaterials*, 2012, **33**, 7794-7802.
44. A. Krueger, Y. Liang, G. Jarre and J. Stegk, *J. Mater. Chem.*, 2006, **16**, 2322-2328.
45. L. Shang, K. Nienhaus and G. U. Nienhaus, *J Nanobiotechnology*, 2014, **12**, 5.
46. M. Ozawa, M. Inaguma, M. Takahashi, F. Kataoka, A. Krüger and E. Ōsawa, *Adv. Mater.*, 2007, **19**, 1201-1206.
47. H. J. Kim, K. Zhang, L. Moore and D. Ho, *ACS Nano*, 2014, **8**, 2998-3005.
48. I. Rehor, J. Slegerova, J. Kucka, V. Proks, V. Petrakova, M.-P. Adam, F. Treussart, S. Turner, S. Bals, P. Sacha, M. Ledvina, A. M. Wen, N. F. Steinmetz and P. Cigler, *Small*, 2014, **10**, 1106-1115.
49. V. Petráková, M. Nesládek, A. Taylor, F. Fendrych, P. Cígler, M. Ledvina, J. Vacík, J. Štursa and J. Kučka, *physica status solidi (a)*, 2011, **208**, 2051-2056.

Table 1: Comparison of Properties of ND-Subtypes

Type	Size (Z-average)	Zeta-potential (mV)	Surface Groups	Synthesis	Citations
dND	45.1 ± 0.2nm[12]	61.2 ± 15.7mV[13]	Alcohol, carboxyl, ketone, aldehyde, anhydride	Detonation of explosives followed by acid washing and ball milling.[46]	Osawa et al.,[46] Chow et al.,[12] Chen et al.,[35] Kim et al.[47]
aND	43.7 ± 0.6nm[13]	46.8 ± 6.89mV[13]	Amine	Reduction of dNDs followed by coupling to (3-aminopropyl)triethoxysilane.[13]	Krueger et al.,[44] Moore et al.,[13] Chow et al.,[12] Zhang et al.[9]
fND	54 ± 7nm[48]	-46.7 ± 5.15mV (not published)	Carboxyl, hydroxyl, ketone	Proton beam irradiation of HPHT NDs followed by annealing at 450 °C.[41]	Havlik et al.,[41] Rehor et al.,[48] Petravka et al.[49]
ND-DNR	93.1 ± 8.2 nm[36]	Not determined	Daunorubicin	Precipitation of dNDs in the presence of daunorubicin and 2.5mM NaOH.[36]	Man et al.[36]

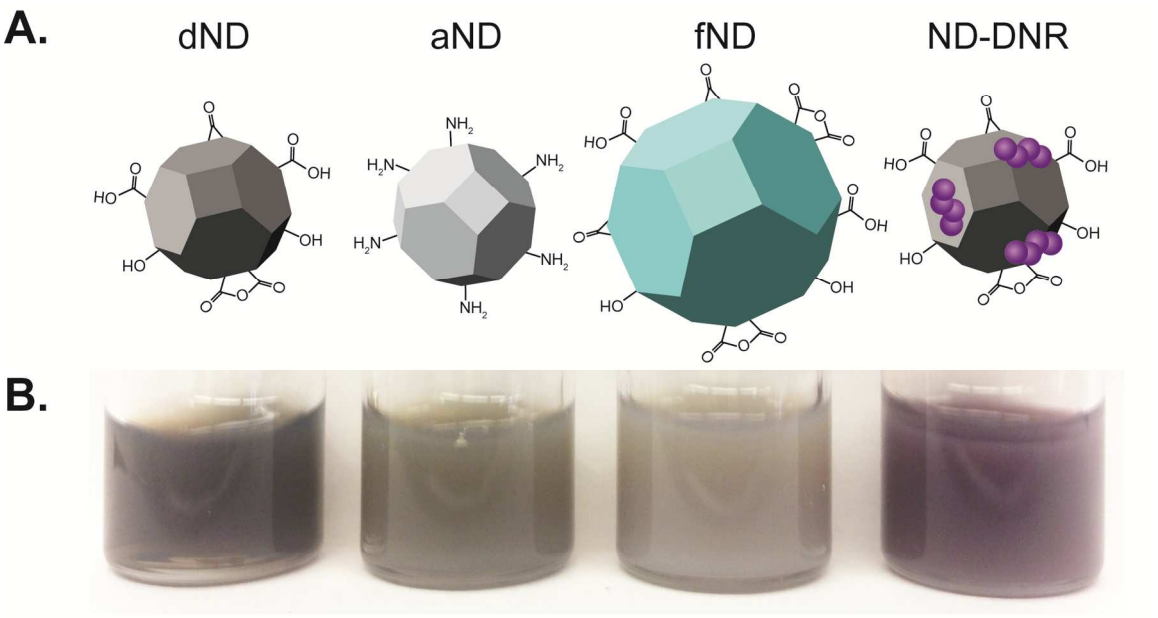

Figure 1: Nanodiamond subtypes. Schematic (A) and photographic (B) comparison of detonation nanodiamonds (dNDs), amine-functionalized detonation nanodiamonds (aNDs), fluorescent nanodiamonds (fNDs) and daunorubicin functionalized detonation nanodiamonds (ND-DNR). Synthesis of dNDs, fNDs and ND-DNR produces NDs with oxygen-containing functional groups while aNDs are generated by reduction of dNDs followed by functionalization to produce primary amines (A). All NDs form stable colloidal solutions in water (B).

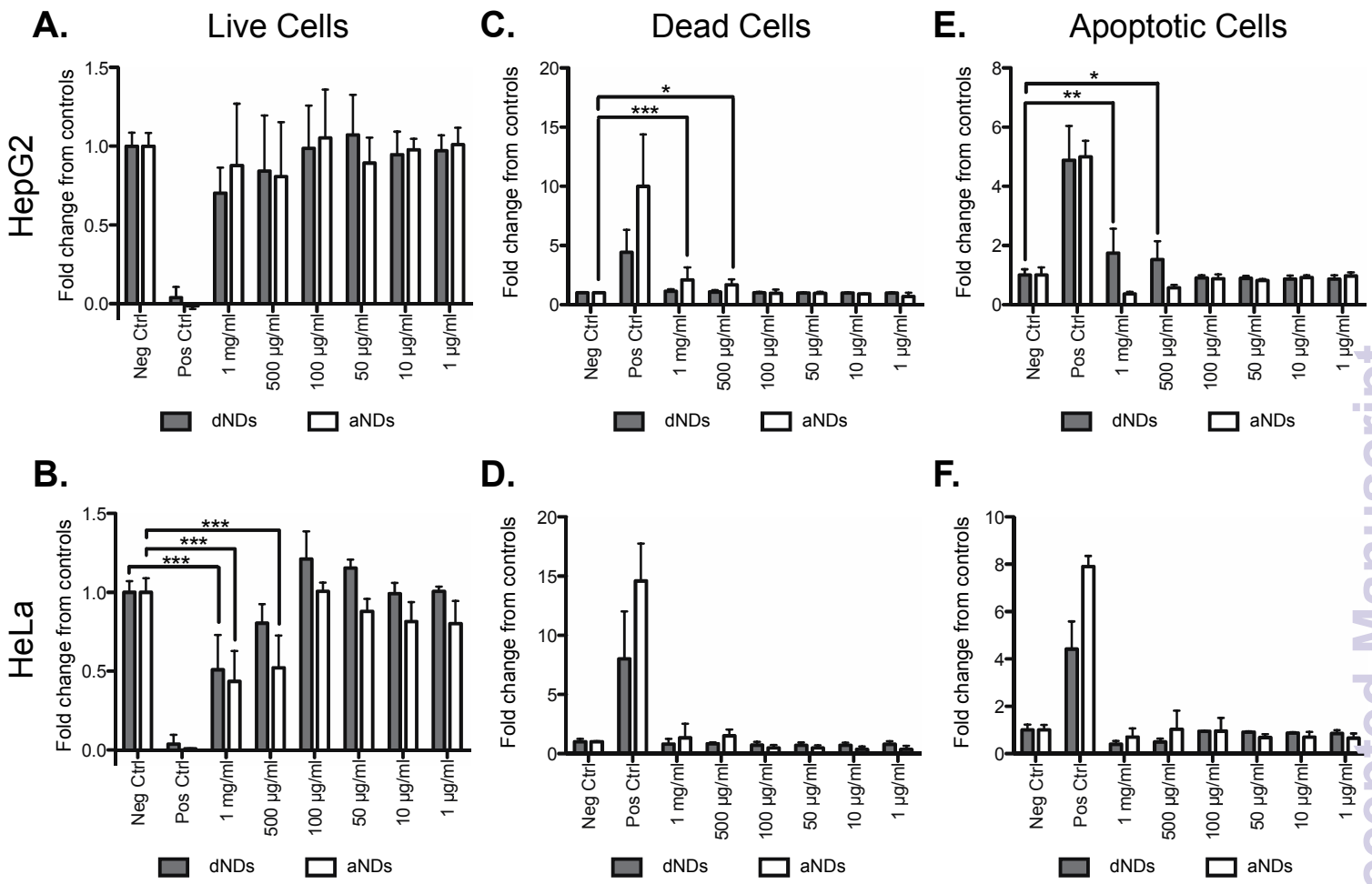

Figure 2: Comparison of unmodified and amine-functionalized detonation NDs. Varying concentrations of NDs were incubated with HepG2 (A, C, E) and HeLa cells (B, D, F) for 24 hours followed by assaying for metabolic activity (XTT; A, B), cell death (lactate dehydrogenase release; C, D) and apoptosis (caspase activity; E, F). Unless otherwise noted all comparisons with negative controls (Neg Ctrl: untreated cells) were non-significant and all comparisons with positive controls (Pos Ctrl: 1% SDS for XTT, assay provided lysis solution for lactate dehydrogenase release and 1-4µM staurosporine for caspase activation) were significant with $p<0.01$ (*$p<0.05$, **$p<0.01$, ***$p<0.001$). Results are expressed as average ± standard deviation of values from a minimum of 3 independent experiments.

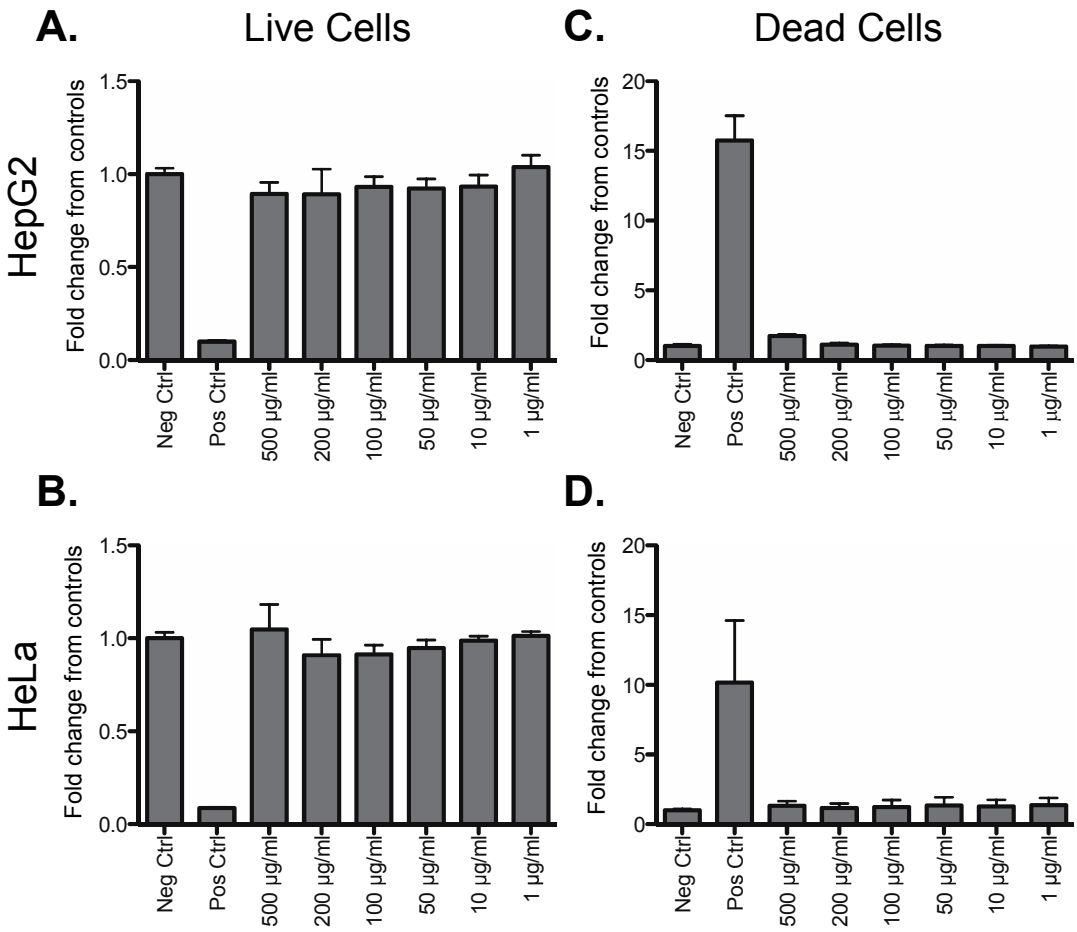

Figure 3: Cellular compatibility of fluorescent NDs. Varying concentrations of fluorescent NDs (fNDs) were incubated with HepG2 (A, C) and HeLa cells (B, D) for 24 hours prior to assaying for metabolic activity (XTT; A, B) and cell death (lactate dehydrogenase release; C, D). All comparisons with negative controls (Neg Ctrl: untreated cells) were non-significant and all comparisons with positive controls (Pos Ctrl: 1% SDS for XTT, assay provided lysis solution for lactate dehydrogenase release and 1-4µM staurosporine for caspase activation) were significant with $p<0.001$. Results are expressed as average ± standard deviation of values from a minimum 3 independent experiments.

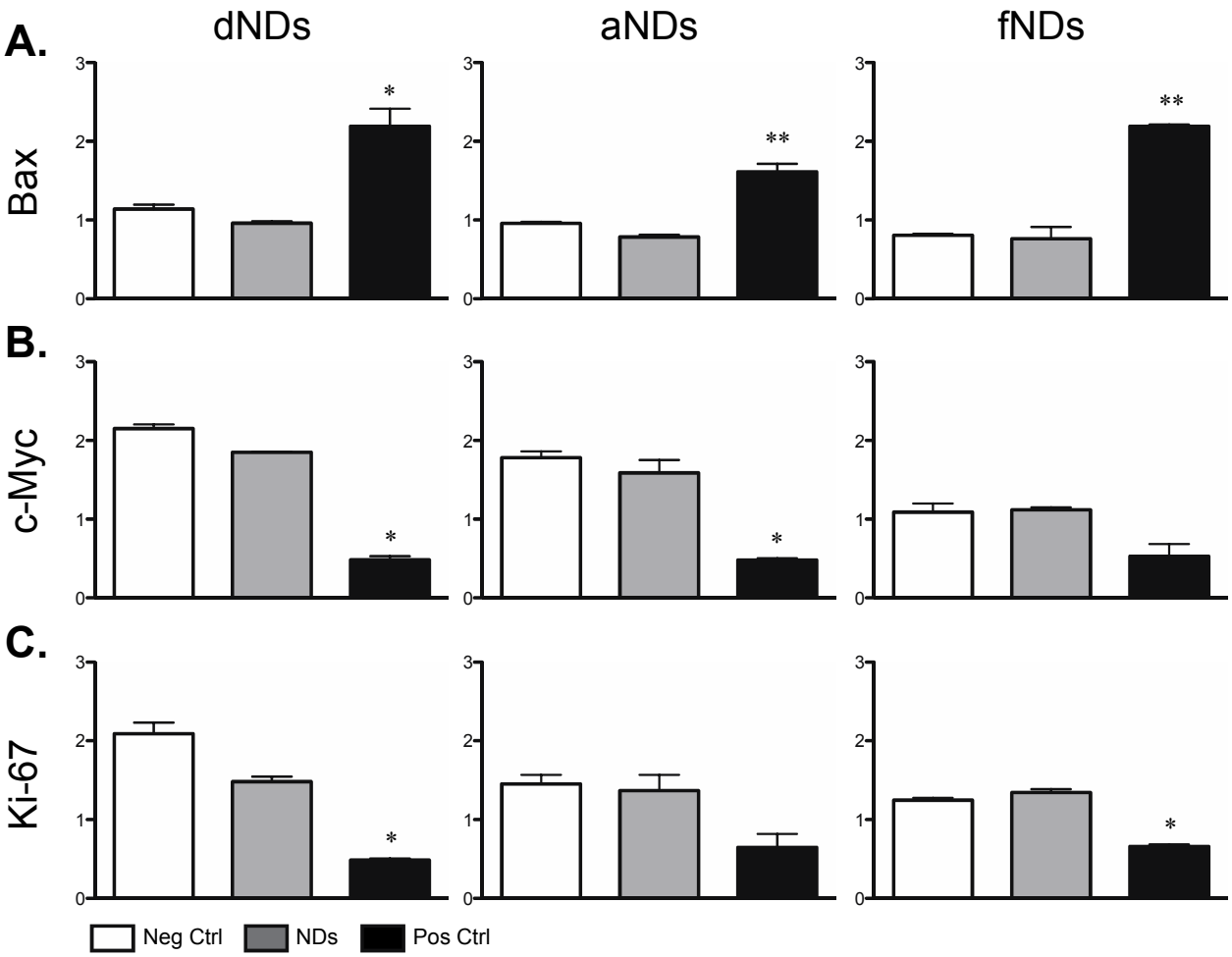

Figure 4: mRNA relative quantification in HepG2 cells after NDs treatment. HepG2 cells were treated with 25 µg/mL of dNDs, aNDs or fNDS for 24 hours prior RT-qPCR analysis of *Bax* (A), *c-Myc* (B) and *Ki-67* (C) genes. Gene expression was normalized to reference gene (*GAPDH*). For *Bax* gene expression analysis was used 1mM Campthotecin as positive control (Pos Ctrl) and for *c-Myc* and *Ki-67* gene expression analysis (5 mg/ml) Campthotecin, respectively. All comparisons between negative control (Neg Ctrl) and NDs were non-significant and comparisons between negative control (Neg Ctrl) and positive control (positive ctrl) were $p<0.05$ or $p<0.01$, respectively (*$p<0.05$, **$p<0.01$, ***$p<0.001$). Results are expressed as average ± standard deviation of values from 3 independent experiments.

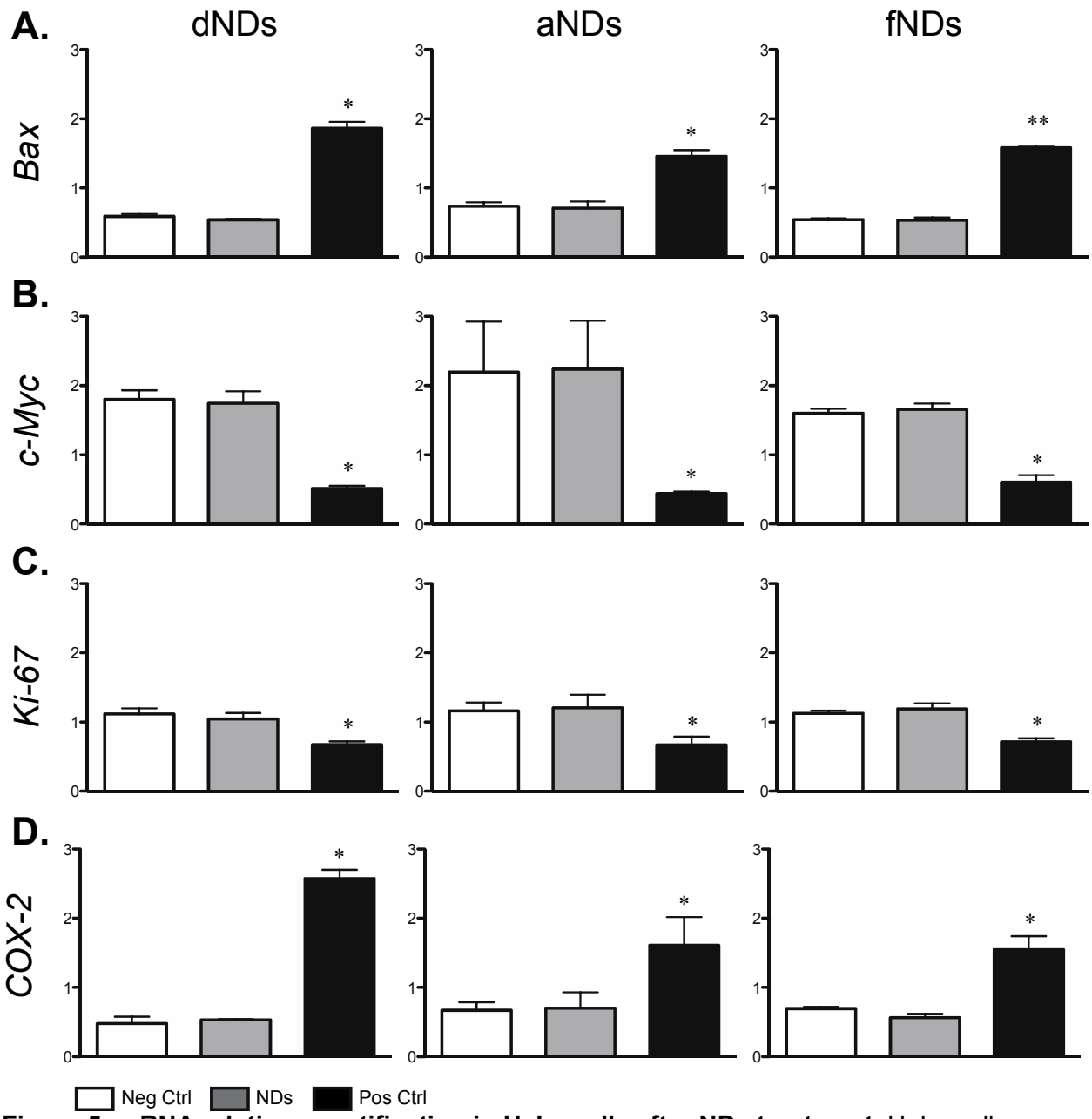

Figure 5: mRNA relative quantification in HeLa cells after NDs treatment. HeLa cells were treated with 25 µg/mL of dNDs, aNDs or fNDS for 24 hours prior qPCR analysis of *Bax* (A), *c-Myc* (B), *Ki-67* (C) and *COX-2* (D) genes. Gene expression was normalized to reference gene (*GAPDH*). For *Bax* and *COX-2* gene expression analysis was used 1mM Campthotecin as positive control (Pos Ctrl) and for *c-Myc* and *Ki-67* gene expression analysis (5 mg/ml) Campthotecin, respectively. All comparisons between negative control (Neg Ctrl) and NDs were non-significant and comparisons between negative control (Neg Ctrl) and positive control (Pos Ctrl) were $p<0.05$ or $p<0.01$, respectively (*$p<0.05$, **$p<0.01$, ***$p<0.001$). Results are expressed as average ± standard deviation of values from 3 independent experiments.

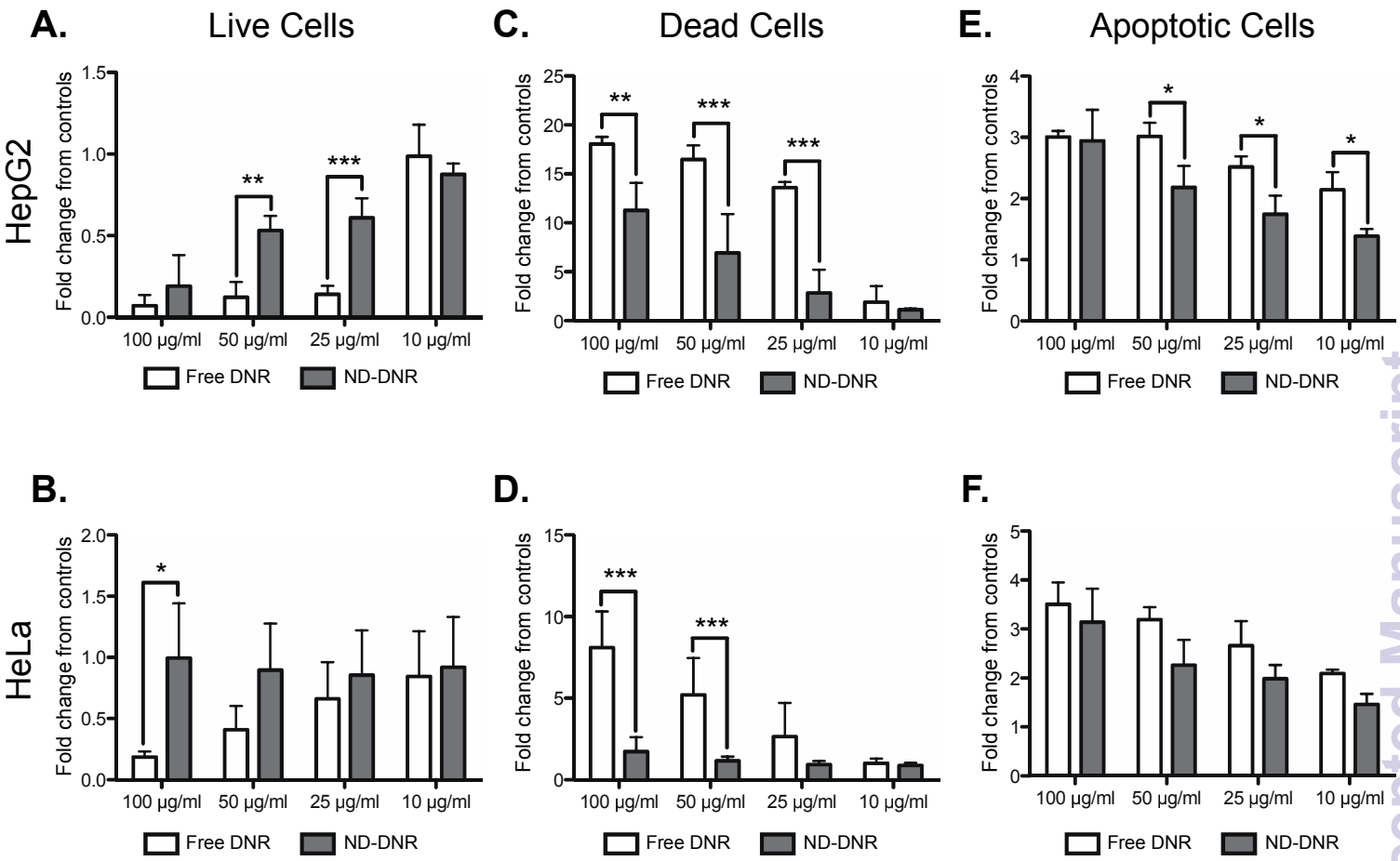

Figure 6: Daunorubicin delivery by detonation NDs. Varying concentrations of Daunorubicin (DNR), either as free drug or loaded on NDs, were incubated with HepG2 (A, C, E) and HeLa cells (B, D, F) for 4 hours followed by assaying for metabolic activity metabolic activity (XTT; A, B), cell death (lactate dehydrogenase release; C, D) and apoptosis (caspase activity; E, F). $p<0.05$ for all ANOVAs (*$p<0.05$, **$p<0.01$, ***$p<0.001$). Results are expressed as average ± standard deviation of values from 3 independent experiments.ś